

## NHERF1/EBP50 Head-to-Tail Intramolecular Interaction Masks Association with PDZ Domain Ligands<sup>∇</sup>

Fabiana C. Morales,<sup>1</sup> Yoko Takahashi,<sup>1</sup> Safan Momin,<sup>1</sup> Henry Adams,<sup>2</sup>  
Xiaomin Chen,<sup>3</sup> and Maria-Magdalena Georgescu<sup>1,2\*</sup>

*Department of Neuro-Oncology,<sup>1</sup> Department of Molecular Genetics,<sup>2</sup> and Department of Biochemistry and Cellular Biology,<sup>3</sup>  
The University of Texas M. D. Anderson Cancer Center, Houston, Texas*

Received 26 July 2006/Returned for modification 9 October 2006/Accepted 9 January 2007

**Loss of cell polarity is one of the initial alterations in the development of human epithelial cancers. Na<sup>+</sup>/H<sup>+</sup> exchanger regulatory factor (NHERF) homologous adaptors 1 and 2 are membrane-associated proteins composed of two amino (N)-terminal PDZ domains and an ezrin-radixin-moesin (ERM)-binding (EB) carboxyl (C)-terminal region. We describe here an intramolecular conformation of NHERF1/EBP50 (ERM-binding phosphoprotein 50) in which the C-terminal EB region binds to the PDZ2 domain. This novel head-to-tail conformation masked the interaction of both PDZ domains with PDZ domain-specific ligands, such as PTEN and  $\beta$ -catenin. An EB region composite structure comprising an  $\alpha$ -helix ending in a PDZ-binding motif imparted opposite effects to NHERF1 associations, mediating binding to ERM proteins and inhibiting binding of PDZ domain ligands. The PDZ domain inhibition was released by prior association of ezrin with the EB region, a condition that occurs in vivo and likely disrupts NHERF1 head-to-tail interaction. In contrast, NHERF2 did not present a regulatory mechanism for protein complex formation. Functionally, NHERF1 is required to organize complexes at the apical membranes of polarized epithelial cells. The regulation of NHERF1 interactions at the apical membrane thus appears to be a dynamic process that is important for maintaining epithelial-tissue integrity.**

Cell polarity is an important characteristic of both unicellular and multicellular organisms and consists of an asymmetry of cell shape and protein distribution that determines the distinct specialized functions of the different parts of the cell cortex. The disruption of epithelial-cell polarity is a critical step for tumor development (reviewed in reference 1). Ezrin, radixin, and moesin (ERM) and neurofibromatosis type 2 (NF2) tumor suppressor compose a subfamily of proteins that belongs to the protein 4.1 superfamily (3). ERM proteins are localized predominantly at the apical membranes of polarized epithelial cells and are known to organize protein complexes that link the membrane to the cytoskeleton. The molecular organization of ERM proteins consists of an amino (N)-terminal FERM (band 4.1, ERM) domain, an extended coiled-coil region, and a short carboxy (C)-terminal domain. Through the FERM domain, ERM proteins bind to transmembrane or membrane-associated proteins, and through their C-terminal domains, they directly interact with actin. ERM proteins form intra- and intermolecular associations by a head-to-tail interaction between their N- and C-terminal domains. The disruption of this interaction by phosphorylation of a conserved residue in the C-terminal domain (T567 in ezrin) represents an important mechanism for promoting the interaction of ERM proteins with other molecules (reviewed in reference 3). One of the main ERM-binding (EB) partners is the adaptor, membrane-associated protein Na<sup>+</sup>/H<sup>+</sup> exchanger (NHE) regulatory factor 1/ERM-binding phosphoprotein 50 (NHERF1/

EBP50). NHERF1 was first characterized as an essential cofactor for cyclic AMP inhibition of Na<sup>+</sup>/H<sup>+</sup> exchange in the rabbit renal brush border membrane (42). ERM proteins bind through their FERM domains to a C-terminal 14-amino-acid EB region of NHERF1 (6). Studies of NHERF1<sup>-/-</sup> mice have shown that NHERF1 is important for stabilizing active phosphorylated ERM proteins at the apical membrane of the polarized epithelia of the kidney and small intestine (24). In addition, NHERF1<sup>-/-</sup> mice present structural defects of the intestinal brush border membrane that resemble defects found in ezrin<sup>-/-</sup> mice (24, 30). A reciprocal destabilization of NHERF1 from the apical membrane of ezrin<sup>-/-</sup> mice was observed, suggesting that the localizations of ezrin and NHERF1 at the apical membrane are interdependent (24, 30).

The N-terminal region of NHERF1 contains two tandem PDZ (postsynaptic-density-95/disc-large/ZO1 homology) domains that bind to the consensus PDZ motif D(S/T)XL (X denotes any residue) present in the C termini of PDZ-interacting proteins (11). Previous studies have shown that the NHERF1 PDZ1 domain binds to a multitude of ligands, including ion transporters, such as type IIa Na/Pi cotransporter (Npt2) (10) and cystic fibrosis transmembrane conductance regulator (11, 35); tyrosine kinase receptors, such as platelet-derived growth factor receptor (PDGFR) (22); and G protein-coupled receptors (GPCRs), such as  $\beta$ 2-adrenergic receptor (12), while the PDZ2 domain binds specifically to  $\beta$ -catenin (34) and Yes-associated protein 65 (23).

A NHERF1 homologous protein, called NHERF2, was identified as being 52% identical and presenting a domain structure similar to that of NHERF1 (43). Despite the similarity between their PDZ domains, NHERF proteins present different affinities for PDZ-binding partners (37). Moreover,

\* Corresponding author. Mailing address: M. D. Anderson Cancer Center, The University of Texas, 6767 Bertner Avenue, Houston, TX 77030. Phone: (713) 834-6201. Fax: (713) 834-6230. E-mail: mgeorges@mdanderson.org.

<sup>∇</sup> Published ahead of print on 22 January 2007.

although NHERF1 and NHERF2 adaptor proteins appear to have functional redundancy, their tissue distributions are distinct. NHERF1 is generally expressed in epithelial tissues co-expressing ezrin, and NHERF2 is coexpressed with moesin and radixin in the alveoli of the lung (16). The renal-proximal tubule cells where NHERF proteins coexist represent an exception to this distinct expression pattern. However, while NHERF1 is expressed apically in association with NHE3, Npt2, and ezrin, NHERF2 is predominantly expressed in the subapical vesicular compartment in these cells (40).

The molecular differences between the NHERF homologous proteins are not well characterized. In the present work, we show that NHERF1 adopts an intramolecular "head-to-tail" folding in which the N-terminal PDZ2 domain interacts with the C-terminal region. This conformation inhibits the association of NHERF1 PDZ domains with PDZ ligands, such as PTEN or  $\beta$ -catenin. The binding of NHERF1 to PDZ ligands was enhanced by prior interaction of the NHERF1 EB region with ERM proteins. Based on these findings, we propose a two-step model in which an initial association between NHERF1 and ERM proteins would unmask NHERF1-PDZ domains for subsequent binding to proteins containing a PDZ motif.

#### MATERIALS AND METHODS

**Plasmids.** Human NHERF1 full-length (FL), splice isoform I2 (24), deletion mutants PDZ1-2, PDZ1iP (PDZ1 plus *inter*-PDZ region), PDZ2-EB in pGEX-6P-1 or in pCMV-2-FLAG vector and NHERF2 FL, and PDZ1-2 and PDZ2-EB in pGEX-6P-1 or pEBG vector were previously described (37). The NHERF1 PDZ motif deletion mutants FL- $\Delta$ SNL and I2- $\Delta$ SNL were obtained by PCR using NHERF1 FL and I2, respectively, as templates. Similarly, the point mutants S290D, F355P, F355R, S356A, L358F, and L354I/L358F were obtained by PCR using NHERF1 FL as a template. All NHERF1 mutants were inserted into pGEX-6P-1 and pCMV-2-FLAG vectors. Npt2, ezrin-N-terminal (NT), PTEN-CT, PDGFR-FL, PDGFR-CT, and EGFR-CT inserted into pGEX-6P-1 or into pGEX-Myc vector were previously described (24, 37), and  $\beta$ -catenin-CT and  $\beta$ -catenin-FL were obtained by PCR from human  $\beta$ -catenin (a gift of Z. Lu) and inserted into the same vectors. The NHERF1 FL, PDZ1-2, PDZ1iP, PDZ2, and EB fragments were inserted into pGEX-Myc for recombinant Myc-tagged protein expression. A fragment encoding the FERM domain of NF2, NF2-NT, was obtained by PCR using mouse NF2 (gift of A. McClatchey) as a template and inserted into pGEX-6P-1 and pGEX-Myc vectors. The His-tagged phosphatase-inactive and phosphorylation-deficient mutant PTEN-C124S-3A and the Myc-tagged constitutively active ezrin- $\Delta$ 53 mutant that lacks the C-terminal 53 residues were inserted into pCDNA vector.

**Cells.** 293T human embryonic kidney cells were grown in Dulbecco modified Eagle's medium supplemented with 10% fetal calf serum. Opossum kidney (OKP) cells (a gift of P. Preisig) were grown in a 1:1 mixture of low-glucose Dulbecco modified Eagle's medium:Ham's F-12 medium supplemented with 10% fetal calf serum (complete growth medium).

**Protein analysis.** The protocols for transfection, cell lysis, Western blotting, glutathione S-transferase (GST) fusion protein purification, pull-down assays with GST fusion proteins, and overlay assays were previously described (8, 37). The pull-down assay of recombinant proteins was performed by incubating for 2 h at 4°C in TNN buffer (50 mM Tris-HCl [pH 7.4], 150 mM NaCl, 5 mM EDTA, and 0.5% NP-40) 5  $\mu$ g of GST fusion proteins with 3  $\mu$ g of recombinant proteins from which the GST tag was previously removed by PreScission protease treatment. The complexes were collected by precipitation with glutathione-agarose beads (Molecular Probes). For GST tag removal, 1 mg recombinant GST fusion protein coupled to 200  $\mu$ l glutathione beads was treated with 0.01 U PreScission protease in 1 ml reaction buffer (50 mM Tris-HCl [pH 7.0], 150 mM NaCl, 1 mM EDTA, 0.01% Tween 20, and 1 mM dithiothreitol) overnight at 4°C. The cleaved protein was recovered from the supernatant with a concentrator column (VivaScience), and the buffer was changed to phosphate-buffered saline. The gel filtration analysis was performed as described previously (24) with minor modifications. Recombinant proteins at various concentrations were loaded on a Sephacryl S300 column (Amersham). The precipitated fractions were resus-

uspended in Laemmli sample buffer and analyzed by Western blotting. For the dimerization studies, recombinant proteins were analyzed by nondenaturing polyacrylamide gel electrophoresis.

For immunoprecipitation, 293T cells cotransfected with either NHERF1-FL, FL- $\Delta$ SNL, or pCMV-2-FLAG vector and PTEN-C124S-3A or ezrin- $\Delta$ 53, were treated with 5 mM dithiobis(succinimidyl)propionate (Pierce) for 30 min at room temperature. The cells were lysed with Triton X-100 buffer (50 mM HEPES [pH 7.5], 100 mM NaCl, 10 mM EDTA, 10% glycerol, and 1% Triton X-100) and processed as described previously (8). All the buffers for protein analysis contained 1 mM phenylmethylsulfonyl fluoride, 21  $\mu$ g/ml aprotinin, 1 mM sodium orthovanadate, and 0.1 mM sodium molybdate. The primary antibodies used were Myc (Invitrogen), Myc (9E10), GST, PTEN (A2B1 and N19) (Santa Cruz Biotechnology), NHERF1 (Calbiochem), and NHERF2 (24). Epitopes on both the PDZ1 and PDZ2 domains are recognized by NHERF1 polyclonal antibody.

**Immunofluorescence analysis.** OKP cells ( $4 \times 10^4$ ) were plated overnight on poly-D-lysine-coated coverslips in complete growth medium. After transfection, the cells were incubated for 48 h to establish polarity, fixed with 3% paraformaldehyde, and processed as described previously (9). The actin cytoskeleton was stained by incubation with rhodamine-labeled phalloidin. Alexa Fluor 488 goat anti-rabbit immunoglobulin G (Molecular Probes) was used as a secondary antibody. Image stacks were acquired on a motorized Nikon TE2000 inverted microscope equipped with a Photometrics CoolSnap HQ charge-coupled device camera (Roper Scientific). Camera and microscope functions were controlled using Metamorph software (Molecular Devices). Autodeblur software (Autoquant) was used to deconvolve the images.

#### RESULTS

**NHERF1 contains a C-terminal PDZ motif that interacts with the PDZ2 domain.** Although NHERF1 interacts strongly with ezrin through the EB region (29), its binding to PDZ domain ligands has been difficult to prove (4, 20, 37). To investigate the possibility that NHERF1 adopts a closed folding in which an intramolecular region binds to its PDZ domains, we analyzed in an overlay assay the combinatorial homotypic interactions between a series of NHERF1 domain mutants (Fig. 1A). These proteins were purified from bacteria fused to GST either with or without a Myc tag. The interaction between the nontagged proteins immobilized on filters and the overlying Myc-tagged proteins present in solution was revealed by subsequently probing the filter with Myc antibody (Fig. 1B). Myc-tagged NHERF1 FL, PDZ1-2, and PDZ2 deletion mutants interacted with NHERF1 domain mutants that had in common the preservation of the EB region (Fig. 1B). Conversely, the Myc-EB mutant interacted with filter-immobilized PDZ1-2 (Fig. 1B, fifth blot). The isolated NHERF1-PDZ1 domain did not by itself establish any homotypic interactions. These experiments showed association between the NHERF1 PDZ2 domain and the EB region.

The examination of the EB region of NHERF1 revealed that its last three amino acids, SNL, conform to the consensus (S/T)XL PDZ motif (11) present in binding partners of NHERF1 PDZ domains (Fig. 1C). To determine whether this motif mediates NHERF1 homotypic association, we overlaid NHERF1-I2 with or without deletion of the last three residues ( $\Delta$ SNL) with Myc-tagged NHERF1 PDZ1-2 protein (Fig. 1D). The deletion completely abolished the association between NHERF1-I2 and PDZ1-2, indicating that the C-terminal PDZ motif is required for the interaction. Moreover, NHERF1 PDZ1-2 preferentially interacted with its own C terminus rather than with the NHERF2 C terminus, in which the C-terminal Leu is replaced by Phe (Fig. 1C and D), underscoring the importance of the consensus PDZ motif sequence for the interaction with NHERF1 PDZ domains.

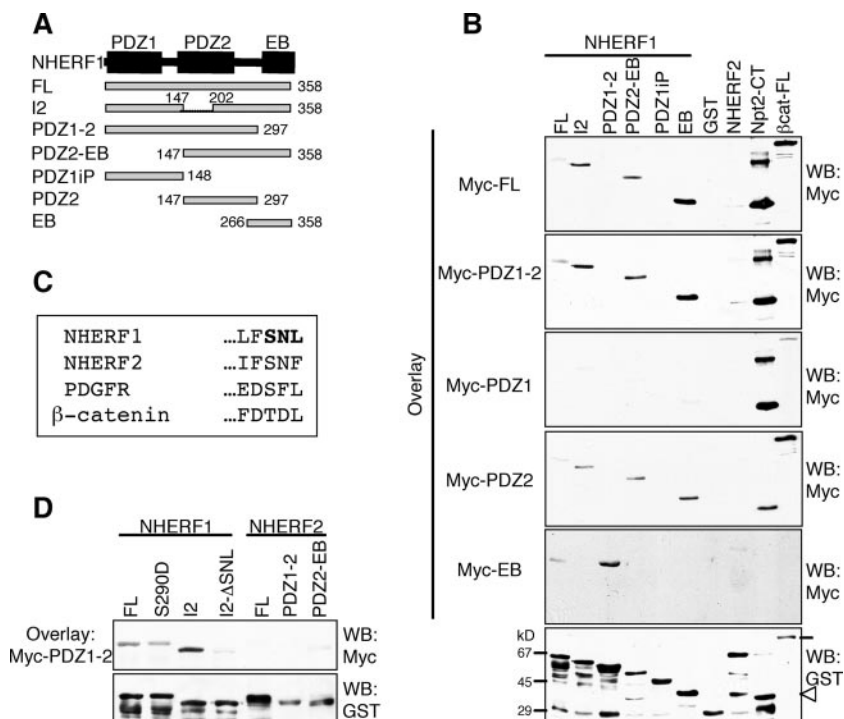


FIG. 1. NHERF1 contains a C-terminal PDZ motif that interacts with the PDZ2 domain. (A) Schematic domain structure of NHERFs showing two tandem PDZ domains (1 and 2) and a C-terminal EB region. Various NHERF1 constructs and their respective amino acid delineation are shown below. (B) Overlay assays showing interaction of overlying Myc-tagged NHERF1 proteins (10  $\mu$ g/ml) with filter-immobilized GST proteins (0.5  $\mu$ g), shown on top of the gels. The interactions were revealed by Western blotting (WB) with Myc antibody. The filters were stripped and reprobbed with GST antibody (bottom). Filter-immobilized GST-Npt2 (arrowhead) and GST- $\beta$ -catenin-FL (line) were used as positive controls for the binding of the NHERF1 PDZ1 and PDZ2 domains, respectively, and GST protein was used as a negative control. (C) Alignment of the C-terminal amino acid sequences of NHERF proteins, PDGFR and  $\beta$ -catenin, that contain a consensus PDZ motif for binding to NHERF1 PDZ domains. Note the C-terminal sequence of NHERF1 (boldface) that conforms to this consensus PDZ motif. (D) Overlay assay showing lack of interaction between overlaid Myc-tagged NHERF1 PDZ1-2 protein and filter-immobilized NHERF1 I2 with the PDZ motif deleted (I2- $\Delta$ SNL) or NHERF2 protein. The assay was performed as for panel B, and filter-immobilized proteins were shown by reprobbed the filter with GST antibody. All experiments were performed at least three times with similar results.

Although NHERF1 Myc-PDZ1-2 interacted well with I2 through the PDZ motif, it interacted poorly with filter-immobilized FL that also contained the PDZ motif (Fig. 1B, second blot, and D). Under the reciprocal conditions, filter-immobilized PDZ1-2 did not interact at all with Myc-FL in solution (Fig. 1B, top blot). These results suggested that the C-terminal PDZ motif is masked in the full-length protein, most likely by intramolecular interaction with the PDZ2 domain. The masking of the PDZ motif depended on the immobilization state of the full-length protein, being partial for the filter-immobilized protein and total for the protein in solution. Conversely, the PDZ2 domain of NHERF1-FL or PDZ2-EB appeared to be masked when these proteins were filter immobilized, as only a breakdown product of NHERF1-FL that had most likely lost the PDZ motif was able to interact with the overlying Myc-EB protein (Fig. 1B, fifth blot). Taken together, these results suggested the presence of an intramolecular "head-to-tail" interaction in NHERF1 that masks the involved regions to various extents, depending on the immobilization state of the protein. To determine whether this head-to-tail interaction could be disrupted by phosphorylation, we generated the S290D phosphorylation-mimicking mutant in the primary constitutive phosphorylation site of NHERF1 (13) and tested its interaction with overlying Myc-PDZ1-2 (Fig. 1D). There was no in-

crease in the interaction between PDZ1-2 and the PDZ motif of S290D compared to FL, indicating that the phosphorylation of Ser 290 had no impact on the intramolecular PDZ domain-PDZ motif association.

**The NHERF1 PDZ motif inhibits the binding of PDZ domain ligands.** Because the PDZ domains of NHERF1 interact with many PDZ motif-containing ligands, we investigated whether these interactions were hindered by the PDZ motif of NHERF1. The specific binding of PTEN to NHERF1 PDZ1 (37) and of  $\beta$ -catenin to PDZ2 (34) was first analyzed by overlay assay of filter-immobilized NHERF1 FL and I2 with or without a PDZ motif (Fig. 2A). Both ligands bound better to the PDZ motif deletion mutant FL- $\Delta$ SNL than to the full-length protein. Moreover, within the same preparation of filter-immobilized full-length NHERF1 protein, both ligands bound better to the low-molecular-weight breakdown products that had most likely lost the EB region than to the intact protein. A concomitant overlay with the ezrin-NT FERM domain showed interaction only with intact EB region-containing proteins (Fig. 2A, compare the upper two blots with the third blot). This experiment suggested that the C-terminal PDZ motif of NHERF1 hindered the interaction between NHERF1 PDZ domains and their specific ligands. To confirm this finding, a GST pull-down assay with the same PDZ domain ligands

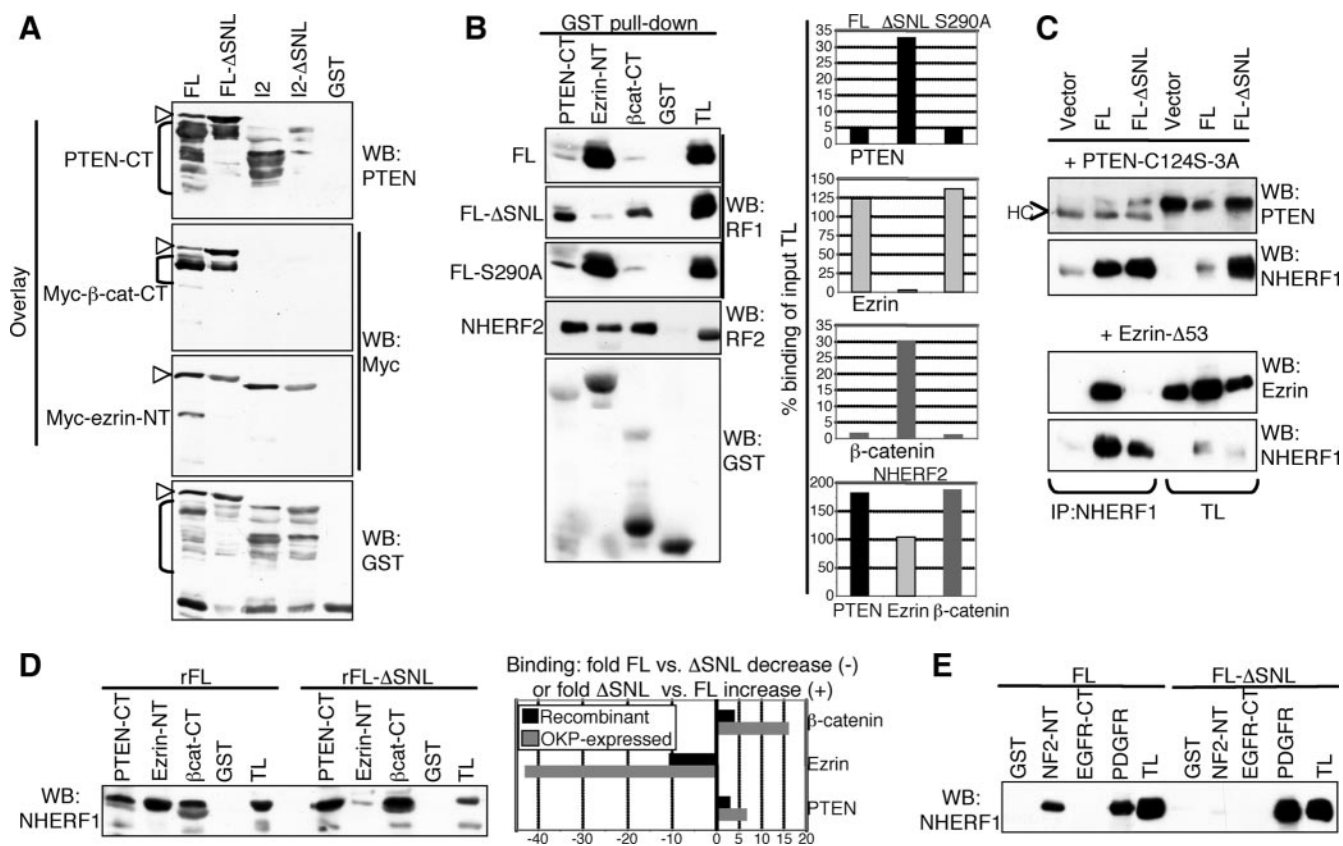


FIG. 2. The NHERF1 PDZ motif prevents the association of ligands with the PDZ domains. (A) The specific associations of PTEN to the NHERF1 PDZ1 domain and of  $\beta$ -catenin to the NHERF1 PDZ2 domain are enhanced by deletion of the PDZ motif ( $\Delta$ SNL) from NHERF1 FL. The filter-immobilized NHERF1 proteins indicated above the filter were overlaid with PTEN-CT, Myc- $\beta$ -catenin-CT, or Myc-ezrin-NT and subsequently probed with PTEN or Myc antibodies to reveal the binding. The amounts of filter-immobilized proteins were exposed by reprobing the filters with GST antibody (bottom). The arrowheads and brackets indicate the intact and the breakdown products of NHERF1 proteins, respectively. (B) GST pull-down assays using the GST fusion proteins (5  $\mu$ g) of PTEN, ezrin, and  $\beta$ -catenin to precipitate protein extracts (0.3 mg) from OKP cells transfected with NHERF1 constructs or NHERF2, as shown on the left. The filters were probed with the antibodies indicated on the right and re-probed with GST antibody. TL, input total lysate (5  $\mu$ g). For the quantitative analysis shown in the graphs, the amounts of precipitated NHERF proteins shown above, with the GST fusion proteins indicated under each graph, were quantified by densitometric analysis using the Image J program (NIH) and are expressed graphically as percentages of the corresponding input total lysate. (C) Coimmunoprecipitation (IP) of PTEN-C124S-3A (top) or of ezrin- $\Delta$ 53 (bottom) with NHERF1 FL and FL- $\Delta$ SNL, following their coexpression in 293T cells. HC represents immunoglobulin heavy chain. Note enhanced or reduced affinity of NHERF1 with the PDZ motif deleted for PTEN or ezrin, respectively. (D) GST pull-down assay, with the same GST fusion proteins as in panel B, of purified recombinant (r) NHERF1 FL and FL- $\Delta$ SNL proteins (3  $\mu$ g) from which the GST moiety was removed. The filters were probed with NHERF1 antibody. The graph shows the comparative analysis of the binding of the GST fusion proteins indicated on the right to NHERF1 proteins either expressed in bacteria (recombinant) or in OKP cells (from the analysis in panel B). The bars represent differences between binding to FL and FL- $\Delta$ SNL for ezrin and between binding to FL- $\Delta$ SNL and FL for PTEN or  $\beta$ -catenin. The levels of NHERF1 precipitated proteins were normalized first by the respective input recombinant protein present in the total lysate (TL). (E) GST pull-down assay with PDZ1 domain ligands (PDGFR and EGFR) and the EB ligand NF2 of NHERF1 FL and FL- $\Delta$ SNL proteins expressed in OKP cells. The filter was probed with NHERF1 antibody.

was performed on NHERF proteins overexpressed in OKP cells (Fig. 2B). Both PDZ domain ligands bound better to NHERF1 when it lacked the C-terminal PDZ motif (Fig. 2B, graphs). In contrast, ezrin association with NHERF1 was profoundly disrupted by the deletion of the PDZ motif. No modification of these interactions was apparent for the NHERF1 phosphorylation-deficient S290A mutant that abolishes the phosphorylation on Ser 290 in mammalian cells, suggesting once more (Fig. 1D) that the phosphorylation of this residue does not modify the configuration of the NHERF1 C-terminal region. In contrast to NHERF1, NHERF2 interacted strongly with PTEN and  $\beta$ -catenin (Fig. 2B), indicating a lack of in-

tramolecular inhibition for PDZ domain ligand binding within this molecule.

Coimmunoprecipitation of proteins overexpressed in 293T cells confirmed that the deletion of the NHERF1 C-terminal PDZ motif enhanced the binding of PTEN and strongly decreased the binding of ezrin to NHERF1 in vivo (Fig. 2C). In vitro, a GST pull-down assay with GST-PTEN, ezrin, and  $\beta$ -catenin on recombinant NHERF1 FL and an FL- $\Delta$ SNL deletion mutant yielded the same results (Fig. 2D). In this assay, which used NHERF1 recombinant proteins, the difference between ligand binding to NHERF1-FL and to  $\Delta$ SNL was not as striking as in the previous GST pull-down assay performed on

NHERF1 proteins expressed in mammalian cells (Fig. 2D, graph). For mammalian-cell-expressed NHERF1 proteins, tighter intramolecular conformational constraints or competitive interaction with proteins from the cellular milieu may explain the more drastic difference from a nonpermissive to a permissive ligand-binding state. This more stringent GST pull-down assay on mammalian-cell-expressed proteins was used to test the consequences of NHERF1 PDZ motif deletion for the association of other NHERF1 PDZ1 domain ligands, such as PDGFR or epidermal growth factor receptor (EGFR), and of another EB-binding ERM member, NF2 (Fig. 2E). While there was no detectable association between NHERF1 and EGFR, confirming our previous results (37), the deletion of the NHERF1 PDZ motif increased the binding of NHERF1 to PDGFR and abolished binding to NF2. These results reinforced the idea that the structural modification induced by NHERF1 PDZ motif deletion rendered the PDZ domains more accessible for interaction with various ligands while it hampered association with ERM proteins.

Because the NHERF proteins were reported to homo- or heterodimerize through their PDZ domains (7, 18, 31), we also analyzed whether the deletion of the NHERF1 PDZ motif modified the dimerization abilities of NHERF1 PDZ domains. As we could not detect homo- or heterodimerization with filter-immobilized proteins (Fig. 1B and D and results not shown), we tested the ability of recombinant NHERF1 to dimerize in solution. Various concentrations of recombinant full-length NHERF1 and a  $\Delta$ SNL deletion mutant were subjected to gel filtration (Fig. 3A). Both proteins eluted in two peaks, a prominent monomeric peak and a second most likely dimeric peak with double the apparent molecular mass of the monomeric peak (Fig. 3A). The dimeric peak was more pronounced for the full-length protein, indicating lower dimerization ability of the C-terminal NHERF1 deletion mutant. Varying the input concentration of the proteins between 0.25 and 1 mg/ml did not significantly alter the elution profile (not shown), indicating stable elution profiles within this concentration range. Similar findings were obtained by electrophoresis on nondenaturing gels, which revealed two NHERF1 bands corresponding to the monomeric and dimeric forms (Fig. 3B). When full-length NHERF1 was preincubated with the ezrin FERM domain, both bands shifted at the expense of a band of intermediate size containing both proteins. The  $\Delta$ SNL deletion mutant appeared to dimerize less and, as expected, did not interact strongly with ezrin. These results suggested that while the conformation change induced by the C-terminal deletion increases NHERF1 PDZ domain ligand binding, it slightly decreases PDZ domain-mediated dimerization ability in solution.

**PDZ domain ligand binding is enhanced by EB region association with ezrin.** Because the EB region interacts with ERM proteins but masks the interaction with PDZ ligands, we tested whether prior engagement of the NHERF1 EB region by the ezrin FERM domain might result in exposure of the PDZ domains. A recombinant Myc-tagged ezrin-NT FERM domain was incubated with NHERF1 FL, and the binding of GST-PTEN-CT and GST- $\beta$ -catenin-CT was tested on the mixture, as well as on NHERF1 FL alone and FL- $\Delta$ SNL as controls (Fig. 4A). The binding of PDZ domain ligands significantly increased when NHERF1 was preincubated with the

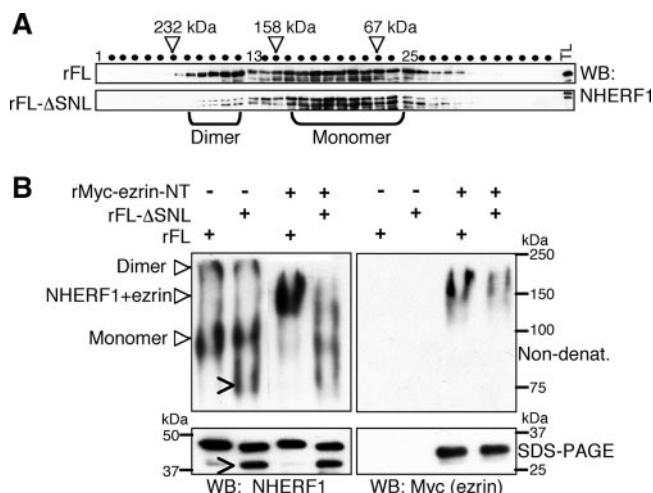


FIG. 3. The NHERF1 PDZ motif enhances dimerization. (A) Gel filtration analysis of NHERF1 FL and FL- $\Delta$ SNL recombinant (r) proteins at 1 mg/ml input protein concentration showing two elution peaks (brackets). The apparent molecular masses are shown above the eluted fractions (dots). Samples were analyzed by Western blotting (WB) using NHERF1 antibody. TL, input total lysate. Note the reduced elution of NHERF1 FL- $\Delta$ SNL in the “dimer peak” compared to the FL protein. (B) The same recombinant proteins as in panel A at 0.1 mg/ml were analyzed either by nondenaturing acrylamide gel electrophoresis (top) or by sodium dodecyl sulfate-polyacrylamide gel electrophoresis (bottom). As a control for homotypic or heterotypic complex formation, both proteins were incubated either separately or with r-Myc-ezrin-NT (1:1 molar ratio) overnight. The filters were probed with NHERF1 antibody (left), stripped, and reprobed with Myc antibody (right) to reveal the complex with Myc-tagged ezrin-NT. The various monomeric or complexed forms are shown with complete arrowheads. A breakdown product of FL- $\Delta$ SNL recombinant protein is shown with open arrowheads. Note dimerization of NHERF1-FL and FL- $\Delta$ SNL proteins and the shift of both FL forms in the ezrin complex. These experiments were performed twice with two freshly prepared recombinant protein stocks for each protein.

ezrin FERM domain. Similar results were obtained by preincubation of the NF2 FERM domain with NHERF1 (not shown). As expected, GST-ezrin-NT competed with prebound Myc-ezrin-NT and associated less with NHERF1 under these conditions (Fig. 4, graph). Although Myc-ezrin-NT did not bind directly to GST-PTEN-CT or to GST- $\beta$ -catenin-CT (not shown), it was precipitated by these proteins in complex with NHERF1 (Fig. 4A, lanes 12 and 14), suggesting the formation of a ternary complex bridged by NHERF1. The small amount of Myc-ezrin-NT precipitated by GST-ezrin-NT via NHERF1 was most likely due to a certain degree of NHERF1 dimerization in solution (Fig. 4A, lane 13). Similar results were obtained by bridging overlay assays in which GST-PTEN-CT and GST- $\beta$ -catenin were immobilized on filters together with GST and GST-NHERF1-FL as negative and positive controls, respectively (Fig. 4B). A first overlay with NHERF1 alone or in a mixture with a nontagged ezrin-NT FERM domain, followed by a second overlay with Myc- $\beta$ -catenin-CT or Myc-ezrin-NT, showed bridging of filter-immobilized proteins to overlaid Myc-tagged proteins only by NHERF1-FL prebound to the ezrin FERM domain (Fig. 4B, compare the blots in columns I and III). In contrast, NHERF2 bridged the complexes irrespective of its prior incubation with the ezrin FERM domain

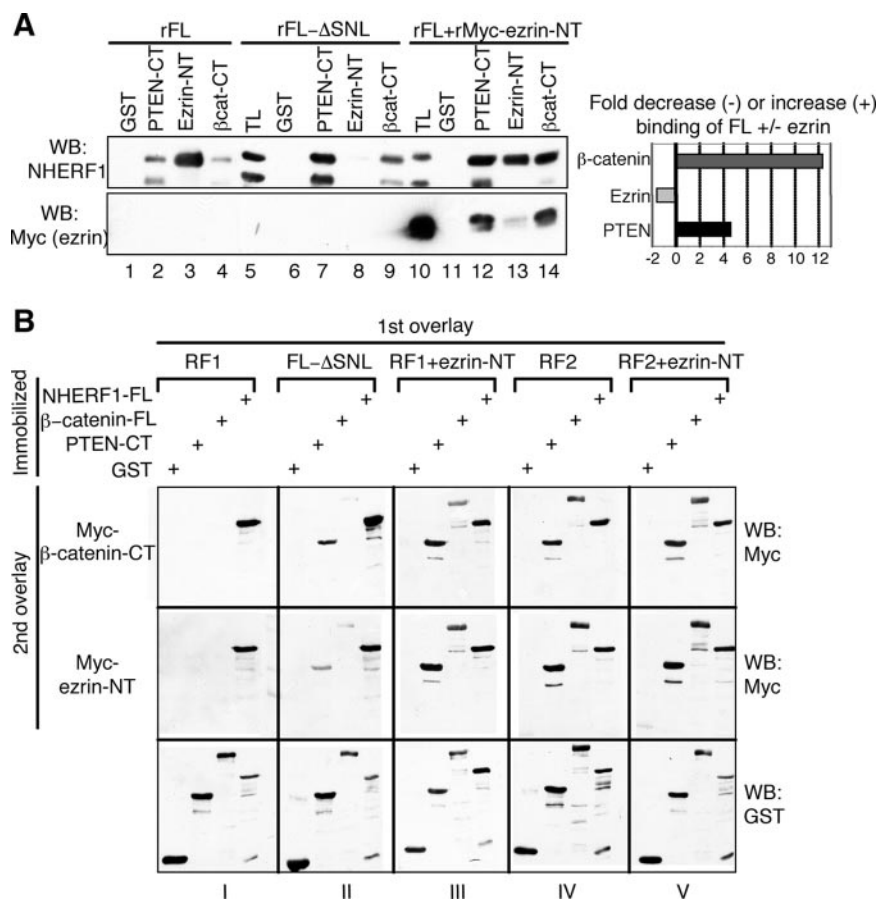


FIG. 4. Prior binding of ezrin to NHERF1 enhances complex formation with PDZ domain ligands. (A) GST pull-down assay with the GST fusion proteins shown above each lane of recombinant (r) NHERF1 FL, FL- $\Delta$ SNL, and FL preincubated overnight with Myc-ezrin-NT at a 1:1 molar ratio. The filters were probed with NHERF1 antibody and reprobbed with Myc antibody to reveal the Myc-tagged ezrin bound to NHERF1. The quantification analysis shown in the graph was performed as for Fig. 2D and represents the difference of binding to NHERF1 in the presence (+) or in the absence (-) of ezrin prebinding to NHERF1. Note the significant enhancement of binding between PTEN or  $\beta$ -catenin and NHERF1 FL by prior interaction of NHERF1 with ezrin. WB, Western blotting. (B) Bridging two-step overlay assays in which the filter-immobilized GST fusion proteins indicated in the top left corner were overlaid in a first step (1st overlay) with NHERF proteins alone or in a mixture (1:1 molar ratio) with ezrin-NT and, in a second step (2nd overlay), with Myc- $\beta$ -catenin-CT or Myc-ezrin-NT. The binding of Myc-tagged  $\beta$ -catenin and ezrin was further revealed by incubation with Myc antibody (right). The filters were stripped and reprobbed with GST antibody. Note that prior interaction with ezrin was required for protein complex bridging by NHERF1 FL (RF1) but not by the NHERF1 FL- $\Delta$ SNL mutant or by NHERF2 FL (RF2).

(Fig. 4B, compare the blots in columns IV and V), suggesting that this molecule is in an "open" conformation state. The slight bridging of Myc- $\beta$ -catenin to filter-immobilized  $\beta$ -catenin by NHERF1 prebound to ezrin or by NHERF2 was due to the dimerization of NHERF proteins in solution (Fig. 4B, blots in columns III to V, first row). As expected, ezrin-NT in the absence of NHERF proteins did not bridge any of these complexes (not shown). These experiments showing increased affinity of NHERF1 for PDZ domain ligands after EB region engagement by ezrin suggested that the association of NHERF1 with ezrin is a mechanism for release of the intramolecular hindrance of NHERF1 PDZ domains.

**Characterization of NHERF1 EB region motifs that influence the associations with PDZ domain ligands and ezrin.** Recently, the crystal structures of the complexes between the radixin FERM domain and NHERF1 or NHERF2 peptide consisting of the last 28 C-terminal residues were solved at 2.5- and 2.8-Å resolution, respectively (38). Under these condi-

tions, the last 11 amino acids of NHERF1 form a three-turn amphipathic  $\alpha$ -helix (Fig. 5A and B) that is required for FERM domain binding (6, 38). This  $\alpha$ -helix includes the terminal PDZ-binding motif that predictably stabilizes the  $\alpha$ -helix, as was also observed from the higher probability value of  $\alpha$ -helix formation for full-length NHERF1 than for a  $\Delta$ SNL mutant (Fig. 5B). The destabilization of the  $\alpha$ -helix in the  $\Delta$ SNL mutant most likely determined the severe impairment of ERM protein binding (Fig. 2B and 5C).

To discriminate between the contributions of the two C-terminal structural elements for NHERF1 PDZ domain masking, we generated point mutations aiming to selectively disrupt the  $\alpha$ -helix and the PDZ motif (Fig. 5A and B). Based on secondary-structure prediction, the mutant F355P disrupts the terminal  $\alpha$ -helix (Fig. 5B). On the other hand, the F355R mutation is predicted to disrupt interaction of the  $\alpha$ -helix with a pocket of the FERM domain (Fig. 5A) and was previously shown to abolish FERM domain binding (6). Both these mu-

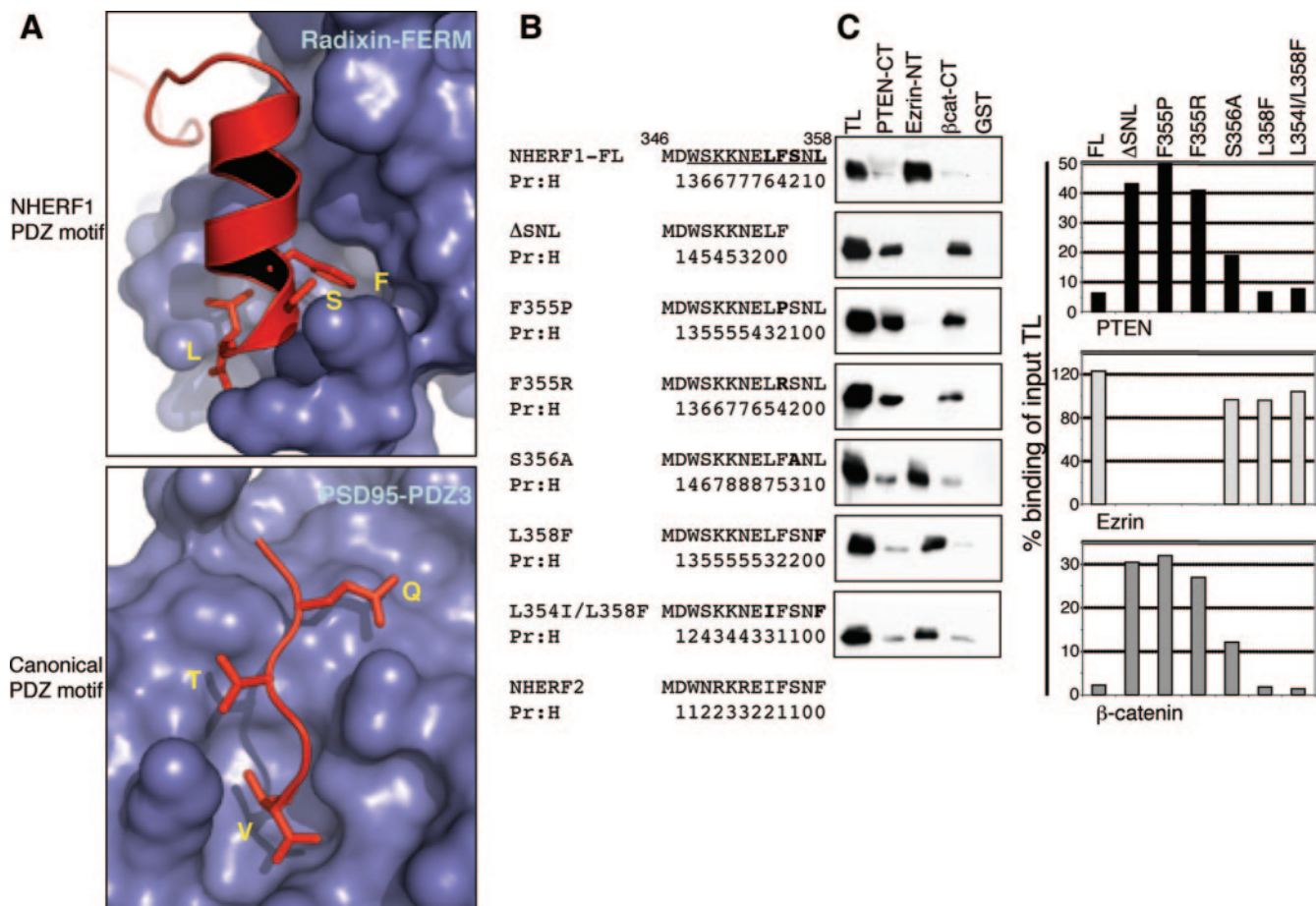


FIG. 5. Structural elements of the NHERF1 C terminus: a terminal  $\alpha$ -helix masks binding to PDZ domain ligands. (A) Comparison of NHERF1 and canonical PDZ motifs. Shown are ribbon models of the NHERF1 EB region docked to the radixin FERM domain and of the CRIPT C-terminal peptide KQTSV bound to the PSD-95 PDZ3 domain. The peptides are shown in red, and the molecular surfaces of domains to which they bind are in blue. For clarity, only the side chains of residues in positions 0, -2, and -3 and the carboxyl group of the last residue are shown as "sticks." These residues are indicated in yellow. Note the contrast between the  $\alpha$ -helical, compressed conformation of the NHERF1 PDZ motif and the linear, extended conformation of the canonical PDZ motif of CRIPT. The figures were generated with the PyMOL program and the Protein Data Bank accession numbers 2D10 (38) and 1BE9 (5). (B) C-terminal amino acid sequence alignment for NHERF1 FL and the indicated mutants and for NHERF2. Mutated residues are shown in boldface. The last 11 residues forming the  $\alpha$ -helix shown in panel A are underlined. The probability of  $\alpha$ -helix prediction (Pr:H) assigned by the program PredictProtein from the European Molecular Biology Laboratory, Heidelberg, Germany, is scaled in numbers from 0 to 9. Note the disruption of the  $\alpha$ -helix by deletion of the PDZ motif. (C) Western blot analysis with NHERF1 antibody of proteins precipitated with PTEN, ezrin, and  $\beta$ -catenin GST fusion proteins (top) from OKP cells transfected with the constructs specified in panel B. The amounts of precipitated NHERF proteins were quantified by densitometric analysis as in Fig. 2B and are expressed graphically as percentages of the corresponding input total lysate (TL).

tations completely abolished the binding of NHERF1 to the ezrin FERM domain and significantly increased the binding of the PDZ domain ligands (Fig. 5C), suggesting that the  $\alpha$ -helix is required for PDZ domain masking. Two types of mutations were also performed in the NHERF1 PDZ motif, a mutation of the consensus (-2) position residue Ser356 to Ala, disrupting the PDZ motif but not the  $\alpha$ -helix, and a mutation changing the last residue, Leu358, to Phe, as in NHERF2 (Fig. 5A and B). The S356A mutation minimally decreased the ezrin FERM domain association, indicative of the integrity of the  $\alpha$ -helix, and only moderately increased the binding of PDZ domain ligands compared to the NHERF1 wild type (Fig. 5C). No significant differences in PDZ domain ligand binding were observed for either L358F or L354I/L358F, changes that mimic the C-terminal sequence of NHERF2 (Fig. 5C), suggesting

that these changes are not sufficient to unmask NHERF1 PDZ domains. Surprisingly, these results indicated that the element important for the masking of NHERF1 PDZ domains is the C-terminal  $\alpha$ -helix rather than the PDZ motif.

The EB region of NHERF1 was shown to be necessary for apical localization of overexpressed NHERF1 in opossum kidney cells, most likely by recruitment of NHERF1 to apically localized endogenous ERM proteins (14). We used this *in vivo* subcellular localization assay to confirm the various degrees of EB region disruption of the NHERF1 mutant proteins (Fig. 6). In agreement with the NHERF1-ezrin association results in Fig. 5C, full-length NHERF1 and the S356A, L358F, and L354I/L358F mutants localized to apical microvilli in the polarized epithelial OKP cells. This finding indicated that all these mutants preserved the terminal  $\alpha$ -helix even if the prob-

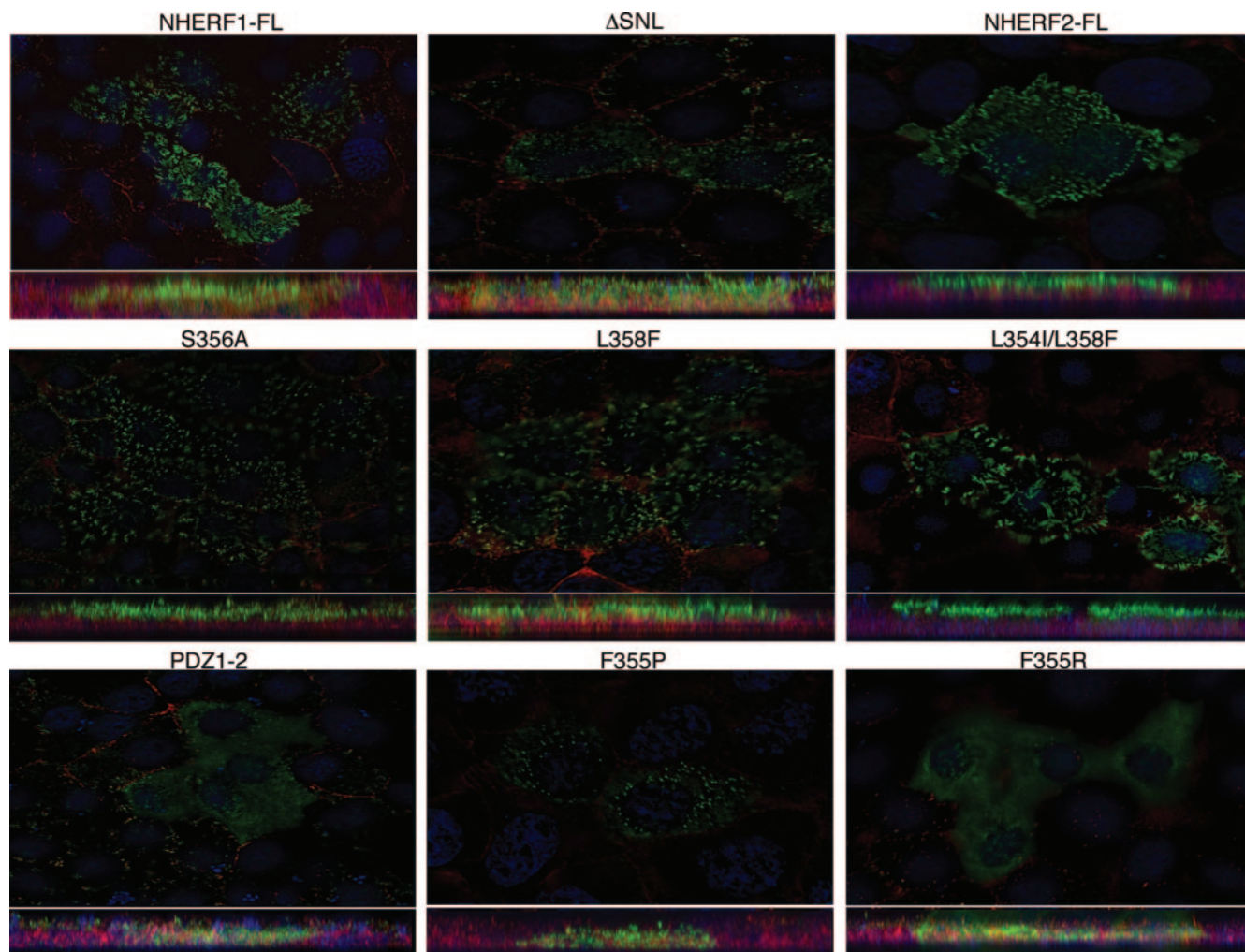


FIG. 6. Subcellular localization of NHERF proteins. Confluent OKP cells plated on poly-D-lysine-coated coverslips were transfected with plasmids encoding the proteins shown above. After fixation, the cells were stained with NHERF1 or NHERF2 antibodies (green) and with DAPI (blue) and rhodamine-labeled phalloidin (red) to expose the nuclei and the actin cytoskeleton, respectively. Images taken with a Nikon TE-200U inverted microscope were deconvolved, and apical sections revealing the microvilli of OKP cells are shown. The XZ sections are shown at the bottom of each image. Note the apical localizations in the microvilli of NHERF1 mutants that preserve the association to ERM proteins.

ability of  $\alpha$ -helix formation was lower for the mutants containing NHERF2 residues (Fig. 5B). The deletion of the NHERF1 PDZ motif largely displaced the  $\Delta$ SNL mutant from the microvilli in the cytoplasm, while the PDZ1-2 deletion mutant and the F355P and F355R point mutants that did not associate with the ezrin FERM domain failed completely to localize apically (Fig. 6). Interestingly, the F355P mutant presented a punctate cytoplasmic staining in comparison to F355R and PDZ1-2. Although the significance of this difference is unknown at present, we speculate, based on the crystal structure and secondary-structure predictions (Fig. 5A and B), that while the F355R change may preserve the folding and amphipathy of the  $\alpha$ -helix, the F355P mutation would entirely disrupt the structure of the  $\alpha$ -helix. These dissimilar changes may distinctly affect the folding and oligomerization state of the whole molecule, with consequences for cytoplasmic distribution and/or reactivity to paraformaldehyde fixation. Overexpressed NHERF2 had an apical localization distinct from that

of NHERF1, reminiscent of the subapical localization in kidney-proximal tubules of the endogenous NHERF2 (40).

## DISCUSSION

The regulated dynamics of association and dissociation of proteins in complexes is a topic of increasing importance, as defects of protein complex formation are responsible for many human pathological conditions, including cancer (27, 28). As a consequence, many therapeutic efforts were recently directed toward the discovery of small molecules inhibiting protein complex formation in signaling pathways that are altered in cancer, the most notorious being the p53/Mdm2 and Wnt/ $\beta$ -catenin pathways (19, 39). The study of adaptor proteins, formed only from modular domains mediating protein-protein interactions, is of particular interest in this respect. NHERF proteins emerged recently as critical adaptors in controlling epithelial-tissue polarity via interaction with ERM proteins (2,



24), metabolic processes via interaction with transmembrane ion transporters (32, 35, 42), and cellular growth via interaction with growth factor receptors and tumor suppressor proteins (22, 25, 34, 37). In this study, we found that NHERF1/EBP50 folds in a head-to-tail conformation that inhibits the interaction of its PDZ domains with ligands. Structurally, the intramolecular interaction took place between the NHERF1 PDZ2 domain and the EB region that ends in a PDZ motif, which was previously described as a consensus PDZ motif for NHERF1 PDZ domain binding (11). Predictably, this folding would engender competition for PDZ2 domain binding between the NHERF1 PDZ motif and the PDZ motifs of heterotypic ligands. Surprisingly, we found that the EB region masked not only the association of the PDZ2 domain with the PDZ2 domain-specific ligand  $\beta$ -catenin, but also the associations of the PDZ1 domain-specific ligands PTEN and PDGFR $\beta$ . Another peculiarity of this intramolecular folding was that although the PDZ motif was required for the homotypic interaction and to some extent for the masking of the PDZ domains, the most important structural element for PDZ domain masking was a C-terminal three-turn  $\alpha$ -helix. This  $\alpha$ -helix is the same structural element of the EB region that mediates binding to ERM proteins (38), and the PDZ motif is embedded in its last half-turn (Fig. 5A). The folding of the NHERF1 PDZ motif thus appears to be unique compared to linear PDZ motifs in other proteins (5) (Fig. 5A), and the nature or even the site of the intramolecular interaction with the PDZ2 domain may very likely be different from those characterizing a classical PDZ motif-PDZ domain interaction, such as the one between the  $\beta$ -catenin PDZ motif and the PDZ2 domain. Although we did not find direct interaction between the EB region and the PDZ1 domain, it is conceivable that PDZ1 participates in the stabilization of intramolecular folding, possibly by making contacts with the C-terminal  $\alpha$ -helix or other EB elements. These contacts would be sufficient to mask the access of linear PDZ motifs to the NHERF1 PDZ1-binding groove (17), explaining the inhibition by the EB region of both PDZ domains' ligand binding. NHERF1 intramolecular folding appeared to inhibit PDZ domain association with PDZ motif-containing ligands and to slightly increase PDZ domain-mediated dimerization. This finding argued for different binding interfaces within NHERF1 PDZ domains for these distinct types of PDZ domain interactions, most likely as in the case of a GRIP1 PDZ6 domain that also engages in homodimerization (15). However, it also pointed out that a more complex structural change than just the PDZ-binding groove masking/unmasking takes place when NHERF1 switches from a "closed" to an "open" conformation. It appears that the open conformation, as induced by prior interaction with ezrin, would favor the interaction with PDZ ligands but not the dimerization. Along this line, we detected NHERF1 dimers containing ezrin only in very small amounts (Fig. 5A). On the other hand, the subsequent interaction of NHERF1 PDZ domains with PDZ ligands might restore the dimerization ability, similarly to the intramolecular closed conformation. This possibility might explain the observed increase of NHERF1 dimerization by prior binding to C-terminal fragments of  $\beta$ 2-adrenergic receptor and PDGFR (18).

Because of the involvement of the NHERF1 EB region in intramolecular folding, we reasoned that the engagement of

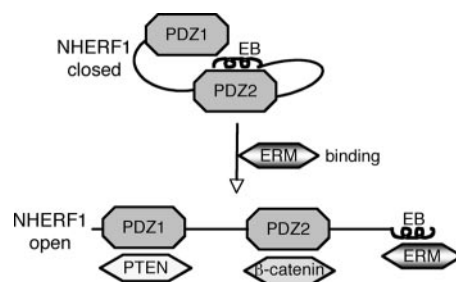


FIG. 7. Model for NHERF1 complex formation with PDZ ligands. NHERF1 presents a "closed" conformation in which the PDZ2 domain binds to the C-terminal EB region in a "head-to-tail" interaction masking the PDZ domains. Engagement of the EB region by ERM proteins switches NHERF1 to an "open" conformation in which the PDZ domains are unmasked and able to bind PDZ domain ligands, represented here by PTEN and  $\beta$ -catenin.

this region by binding to ERM proteins would open the molecule and allow access by PDZ domain ligands. Accordingly, we characterized a mechanism for unmasking the PDZ domains by prior interaction of the NHERF1 EB region with ERM proteins (Fig. 7). Preincubation of NHERF1 with ezrin completely unmasked the PDZ domains for heterotypic ligand binding and allowed the assembly of various protein complexes containing both ezrin and PDZ domain ligands. In vitro, we could distinguish ternary complexes containing ezrin and one PDZ domain ligand that were bridged mainly by single NHERF1 molecules. In overlay assays, we could even show that NHERF1 prebound to ezrin could assemble PDZ domain ligands to both PDZ domains, most likely on single NHERF1 molecules (Fig. 5B). This diversity of protein complexes triggered by a prior interaction between NHERF1 and ezrin suggested a possible model *in vivo* in which the high-affinity binding between NHERF1 and ERM proteins at the plasma membrane (24, 26, 29) would engender unmasking of NHERF1 PDZ domains and subsequent recruitment of intracellular ligands, such as PTEN or  $\beta$ -catenin, to the cortical compartment or strong binding of NHERF1 to transmembrane PDZ domain ligands, such as PDGFR, GPCRs, or ion transporters. In these cortical complexes, NHERF1 would regulate or stabilize its PDZ domain ligands (33). In support of this hypothesis, the presence of the EB region was found to be necessary for the regulation and membrane stabilization of transmembrane ion transporters and GPCRs by NHERF1 (21, 36, 41).

In contrast to NHERF1, NHERF2 interacted well with PDZ domain ligands, to an even greater degree than with ezrin. In the absence of ezrin prebinding, NHERF2 could assemble complexes containing PDZ domain ligands to extents similar to those of NHERF1 prebound to ezrin (Fig. 4B). Furthermore, the ability of NHERF2 to form complexes was not enhanced by prior interaction with ezrin, suggesting that NHERF2 is in an "open" conformation and that the binding of ezrin does not regulate its ability to interact with PDZ domain ligands. A possibility explaining the difference in intramolecular folding between the NHERF proteins could be that the EB region of NHERF2, which differs by several residues from that of NHERF1 (Fig. 5B), does not mask the PDZ domains. However, both EB regions were reported to form the C-terminal three-turn  $\alpha$ -helix (38) that we showed to be necessary for

PDZ domain masking, and the swapping of one or two residues from NHERF2 to the NHERF1 PDZ motif and  $\alpha$ -helix did not unmask NHERF1 PDZ domains or change NHERF1 subcellular localization. Perhaps these changes were not sufficient to disrupt NHERF1 intramolecular folding, and a more extensive swap of the EB region might be necessary to achieve this effect. The fact that we did not detect binding between NHERF1 PDZ1-2 and NHERF2 constructs containing the whole EB region (Fig. 1D) favors this possibility. Another possibility is that the conformations of the PDZ domains differ in the two proteins and NHERF2 PDZ domains are less prone to entail a head-to-tail interaction. We have previously shown that the PDZ domains of NHERF1 and NHERF2 are not equivalent and that ligands of the NHERF1 PDZ1 domain have higher affinity for the NHERF2 PDZ2 domain (37). Regardless of the affinities of individual PDZ domains for ligands, the difference in ligand accessibility to the PDZ domains and the possibility to regulate this accessibility in NHERF1 suggest important functional differences between the two NHERF proteins. While NHERF2 may constitutively interact with PDZ domain ligands, the controlled interaction of NHERF1 with PDZ domain ligands may implicate NHERF1 in more dynamic processes, such as trafficking.

Although intramolecular head-to-tail inhibitory conformations have been described for many molecules, including the ERM proteins (3), this is the first such folding involving PDZ domains. Because of the novel features of NHERF1 intramolecular interaction, most likely involving both PDZ domains and at least two structural elements of the EB region, solving the three-dimensional structure of the full-length molecule appears to be an important step in elucidating these interactions. Moreover, this approach will shed light on the mechanism of PDZ domain masking, providing important insights for the development of PDZ domain-blocking drugs for cancer therapy.

#### ACKNOWLEDGMENTS

We are indebted to T. J. Liu for insightful discussions and to Avani Verma for help with protein purification.

This work was supported by awards from the Goldhirsh Foundation and the University of Texas M. D. Anderson Cancer Center Tobacco Fund and NCI-CA107201 to M.-M.G. and from the American Brain Tumor Association to F.C.M. The DNA sequencing and the animal breeding were partially supported by NCI-CA16672.

#### REFERENCES

- Bissell, M. J., and D. Radisky. 2001. Putting tumours in context. *Nat. Rev. Cancer* **1**:46–54.
- Bretscher, A., D. Chambers, R. Nguyen, and D. Reczek. 2000. ERM-Merlin and EBP50 protein families in plasma membrane organization and function. *Annu. Rev. Cell Dev. Biol.* **16**:113–143.
- Bretscher, A., K. Edwards, and R. G. Fehon. 2002. ERM proteins and merlin: integrators at the cell cortex. *Nat. Rev. Mol. Cell. Biol.* **3**:586–599.
- Dai, J. L., L. Wang, A. A. Sahin, L. D. Broemeling, M. Schutte, and Y. Pan. 2004. NHERF (Na<sup>+</sup>/H<sup>+</sup> exchanger regulatory factor) gene mutations in human breast cancer. *Oncogene* **23**:8681–8687.
- Doyle, D. A., A. Lee, J. Lewis, E. Kim, M. Sheng, and R. MacKinnon. 1996. Crystal structures of a complexed and peptide-free membrane protein-binding domain: molecular basis of peptide recognition by PDZ. *Cell* **85**:1067–1076.
- Finnerty, C. M., D. Chambers, J. Ingraffea, H. R. Faber, P. A. Karplus, and A. Bretscher. 2004. The EBP50-moesin interaction involves a binding site regulated by direct masking on the FERM domain. *J. Cell Sci.* **117**:1547–1552.
- Fouassier, L., C. C. Yun, J. G. Fitz, and R. B. Doctor. 2000. Evidence for ezrin-radixin-moesin-binding phosphoprotein 50 (EBP50) self-association through PDZ-PDZ interactions. *J. Biol. Chem.* **275**:25039–25045.
- Georgescu, M. M., K. H. Kirsch, T. Akagi, T. Shishido, and H. Hanafusa. 1999. The tumor-suppressor activity of PTEN is regulated by its carboxyl-terminal region. *Proc. Natl. Acad. Sci. USA* **96**:10182–10187.
- Georgescu, M. M., K. H. Kirsch, P. Kaloudis, H. Yang, N. P. Pavletich, and H. Hanafusa. 2000. Stabilization and productive positioning roles of the C2 domain of PTEN tumor suppressor. *Cancer Res.* **60**:7033–7038.
- Gisler, S. M., I. Stagljar, M. Traebert, D. Bacic, J. Biber, and H. Murer. 2001. Interaction of the type IIa Na/Pi cotransporter with PDZ proteins. *J. Biol. Chem.* **276**:9206–9213.
- Hall, R. A., L. S. Ostedgaard, R. T. Premont, J. T. Blitzer, N. Rahman, M. J. Welsh, and R. J. Lefkowitz. 1998. A C-terminal motif found in the  $\beta$ 2-adrenergic receptor, P2Y1 receptor and cystic fibrosis transmembrane conductance regulator determines binding to the Na<sup>+</sup>/H<sup>+</sup> exchanger regulatory factor family of PDZ proteins. *Proc. Natl. Acad. Sci. USA* **95**:8496–8501.
- Hall, R. A., R. T. Premont, C. W. Chow, J. T. Blitzer, J. A. Pitcher, A. Claing, R. H. Stoffel, L. S. Barak, S. Shenolikar, E. J. Weinman, S. Grinstein, and R. J. Lefkowitz. 1998. The  $\beta$ 2-adrenergic receptor interacts with the Na<sup>+</sup>/H<sup>+</sup>-exchanger regulatory factor to control Na<sup>+</sup>/H<sup>+</sup> exchange. *Nature* **392**:626–630.
- Hall, R. A., R. F. Spurney, R. T. Premont, N. Rahman, J. T. Blitzer, J. A. Pitcher, and R. J. Lefkowitz. 1999. G protein-coupled receptor kinase 6A phosphorylates the Na<sup>+</sup>/H<sup>+</sup> exchanger regulatory factor via a PDZ domain-mediated interaction. *J. Biol. Chem.* **274**:24328–24334.
- Hernando, N., N. Deliot, S. M. Gisler, E. Lederer, E. J. Weinman, J. Biber, and H. Murer. 2002. PDZ-domain interactions and apical expression of type IIa Na/Pi cotransporters. *Proc. Natl. Acad. Sci. USA* **99**:11957–11962.
- Im, Y. J., S. H. Park, S. H. Rho, J. H. Lee, G. B. Kang, M. Sheng, E. Kim, and S. H. Eom. 2003. Crystal structure of GRIP1 PDZ6-peptide complex reveals the structural basis for class II PDZ target recognition and PDZ domain-mediated multimerization. *J. Biol. Chem.* **278**:8501–8507.
- Ingraffea, J., D. Reczek, and A. Bretscher. 2002. Distinct cell type-specific expression of scaffolding proteins EBP50 and E3KARP: EBP50 is generally expressed with ezrin in specific epithelia, whereas E3KARP is not. *Eur. J. Cell Biol.* **81**:61–68.
- Karthikeyan, S., T. Leung, G. Birrane, G. Webster, and J. A. Ladias. 2001. Crystal structure of the PDZ1 domain of human Na<sup>+</sup>/H<sup>+</sup> exchanger regulatory factor provides insights into the mechanism of carboxyl-terminal leucine recognition by class I PDZ domains. *J. Mol. Biol.* **308**:963–973.
- Lau, A. G., and R. A. Hall. 2001. Oligomerization of NHERF-1 and NHERF-2 PDZ domains: differential regulation by association with receptor carboxyl-termini and by phosphorylation. *Biochemistry* **40**:8572–8580.
- Lepourcelet, M., Y. N. Chen, D. S. France, H. Wang, P. Crews, F. Petersen, C. Bruseo, A. W. Wood, and R. A. Shivdasani. 2004. Small-molecule antagonists of the oncogenic Tcf/ $\beta$ -catenin protein complex. *Cancer Cell* **5**:91–102.
- Li, C., K. Roy, K. Dandridge, and A. P. Naren. 2004. Molecular assembly of cystic fibrosis transmembrane conductance regulator in plasma membrane. *J. Biol. Chem.* **279**:24673–24684.
- Li, J. G., C. Chen, and L. Y. Liu-Chen. 2002. Ezrin-radixin-moesin-binding phosphoprotein-50/Na<sup>+</sup>/H<sup>+</sup> exchanger regulatory factor (EBP50/NHERF) blocks U50,488H-induced down-regulation of the human kappa opioid receptor by enhancing its recycling rate. *J. Biol. Chem.* **277**:27545–27552.
- Maudsley, S., A. M. Zamah, N. Rahman, J. T. Blitzer, L. M. Luttrell, R. J. Lefkowitz, and R. A. Hall. 2000. Platelet-derived growth factor receptor association with Na<sup>+</sup>/H<sup>+</sup> exchanger regulatory factor potentiates receptor activity. *Mol. Cell. Biol.* **20**:8352–8363.
- Mohler, P. J., S. M. Kreda, R. C. Boucher, M. Sudol, M. J. Stutts, and S. L. Milgram. 1999. Yes-associated protein 65 localizes p62(c-Yes) to the apical compartment of airway epithelia by association with EBP50. *J. Cell Biol.* **147**:879–890.
- Morales, F. C., Y. Takahashi, E. L. Kreimann, and M.-M. Georgescu. 2004. Ezrin-radixin-moesin (ERM)-binding phosphoprotein 50 organizes ERM proteins at the apical membrane of polarized epithelia. *Proc. Natl. Acad. Sci. USA* **101**:17705–17710.
- Murthy, A., C. Gonzalez-Agosti, E. Cordero, D. Pinney, C. Candia, F. Solomon, J. Gusella, and V. Ramesh. 1998. NHE-RF, a regulatory cofactor for Na<sup>+</sup>/H<sup>+</sup> exchange, is a common interactor for merlin and ERM (MERM) proteins. *J. Biol. Chem.* **273**:1273–1276.
- Nguyen, R., D. Reczek, and A. Bretscher. 2001. Hierarchy of merlin and ezrin N- and C-terminal domain interactions in homo- and heterotypic associations and their relationship to binding of scaffolding proteins EBP50 and E3KARP. *J. Biol. Chem.* **276**:7621–7629.
- Noury, C., S. G. Grant, and J. P. Borg. 2003. PDZ domain proteins: plug and play! *Sci. STKE* **2003**:RE7.
- Pawson, T., and P. Nash. 2003. Assembly of cell regulatory systems through protein interaction domains. *Science* **300**:445–452.
- Reczek, D., M. Berryman, and A. Bretscher. 1997. Identification of EBP50: a PDZ-containing phosphoprotein that associates with members of the ezrin-radixin-moesin family. *J. Cell Biol.* **139**:169–179.
- Saotome, I., M. Curto, and A. I. McClatchey. 2004. Ezrin is essential for epithelial organization and villus morphogenesis in the developing intestine. *Dev. Cell* **6**:855–864.

31. **Shenolikar, S., C. M. Minkoff, D. A. Steplock, C. Evangelista, M. Liu, and E. J. Weinman.** 2001. N-terminal PDZ domain is required for NHERF dimerization. *FEBS Lett.* **489**:233–236.
32. **Shenolikar, S., J. W. Voltz, C. M. Minkoff, J. B. Wade, and E. J. Weinman.** 2002. Targeted disruption of the mouse NHERF-1 gene promotes internalization of proximal tubule sodium-phosphate cotransporter type IIa and renal phosphate wasting. *Proc. Natl. Acad. Sci. USA* **99**:11470–11475.
33. **Shenolikar, S., and E. J. Weinman.** 2001. NHERF: targeting and trafficking membrane proteins. *Am. J. Physiol.* **280**:F389–F395.
34. **Shibata, T., M. Chuma, A. Kokubu, M. Sakamoto, and S. Hirohashi.** 2003. EBP50, a beta-catenin-associating protein, enhances Wnt signaling and is over-expressed in hepatocellular carcinoma. *Hepatology* **38**:178–186.
35. **Short, D. B., K. W. Trotter, D. Reczek, S. M. Kreda, A. Bretscher, R. C. Boucher, M. J. Stutts, and S. L. Milgram.** 1998. An apical PDZ protein anchors the cystic fibrosis transmembrane conductance regulator to the cytoskeleton. *J. Biol. Chem.* **273**:19797–19801.
36. **Sneddon, W. B., C. A. Syme, A. Bisello, C. E. Magyar, M. D. Rochdi, J. L. Parent, E. J. Weinman, A. B. Abou-Samra, and P. A. Friedman.** 2003. Activation-independent parathyroid hormone receptor internalization is regulated by NHERF1 (EBP50). *J. Biol. Chem.* **278**:43787–43796.
37. **Takahashi, Y., F. C. Morales, E. L. Kreimann, and M. M. Georgescu.** 2006. PTEN tumor suppressor associates with NHERF proteins to attenuate PDGF receptor signaling. *EMBO J.* **25**:910–920.
38. **Terawaki, S., R. Maesaki, and T. Hakoshima.** 2006. Structural basis for NHERF recognition by ERM proteins. *Structure* **14**:777–789.
39. **Vassilev, L. T., B. T. Vu, B. Graves, D. Carvajal, F. Podlaski, Z. Filipovic, N. Kong, U. Kammlott, C. Lukacs, C. Klein, N. Fotouhi, and E. A. Liu.** 2004. In vivo activation of the p53 pathway by small-molecule antagonists of MDM2. *Science* **303**:844–848.
40. **Wade, J. B., J. Liu, R. A. Coleman, R. Cunningham, D. A. Steplock, W. Lee-Kwon, T. L. Pallone, S. Shenolikar, and E. J. Weinman.** 2003. Localization and interaction of NHERF isoforms in the renal proximal tubule of the mouse. *Am. J. Physiol. Cell Physiol.* **285**:C1494–C1503.
41. **Weinman, E. J., D. Steplock, M. Donowitz, and S. Shenolikar.** 2000. NHERF associations with sodium-hydrogen exchanger isoform 3 (NHE3) and ezrin are essential for cAMP-mediated phosphorylation and inhibition of NHE3. *Biochemistry* **39**:6123–6129.
42. **Weinman, E. J., D. Steplock, Y. Wang, and S. Shenolikar.** 1995. Characterization of a protein cofactor that mediates protein kinase A regulation of the renal brush border membrane Na<sup>+</sup>-H<sup>+</sup> exchanger. *J. Clin. Investig.* **95**:2143–2149.
43. **Yun, C. H., S. Oh, M. Zizak, D. Steplock, S. Tsao, C. M. Tse, E. J. Weinman, and M. Donowitz.** 1997. cAMP-mediated inhibition of the epithelial brush border Na<sup>+</sup>/H<sup>+</sup> exchanger, NHE3, requires an associated regulatory protein. *Proc. Natl. Acad. Sci. USA* **94**:3010–3015.